FERMILAB-Pub-96/033-T
IPNO/TH 96-09

# Dispersive Approach to Semileptonic Form-Factors in Heavy-to-Light Meson Decays

**Gustavo Burdman**
*Fermi National Accelerator Laboratory, Batavia, Illinois 60510, USA.*

**Joachim Kambor**
*Division de Physique Théorique*[1]*, Institut de Physique Nucléaire*
*F–91406 Orsay Cedex, France.*

**Abstract**

We study the semileptonic decays of heavy mesons into light pseudoscalars by making use of dispersion relations. Constraints from heavy quark symmetry, chiral symmetry and perturbative QCD are implemented into a dispersive model for the form-factors. Large deviations from $B^*$-pole dominance are observed in $B \to \pi\ell\nu$. We discuss the model prediction for this mode and its possible impact on the extraction of $|V_{ub}|$.

[1]Unité de Recherche des Universités Paris XI et Paris VI associé au CNRS.

# 1 Introduction

Semileptonic decays of heavy hadrons are of great interest given that they are the cleanest way to probe the mixing between quarks of the third generation with those of the lighter families. The extraction of the Cabibbo-Kobayashi-Maskawa (CKM) matrix element $V_{cb}$ from the $b \to c\ell\nu$ transitions is largely freed from theoretical uncertainties since the advent of the heavy quark symmetries [1]. This is the case for exclusive decays [2] as well as for the inclusive lepton spectrum [3]. On the other hand, the $b \to u\ell\nu$ transitions involving the CKM element $V_{ub}$ are still plagued with large theoretical uncertainties. The inclusive lepton spectrum above the $b \to c\ell\nu$ end-point, from which $|V_{ub}|/|V_{cb}|$ can be extracted, is still the realm of models due to the breakdown of the heavy quark operator product expansion. For the exclusive decays, the use of heavy quark symmetry (HQS) is reduced to relating the $D$ and $B$ decays to light hadrons at fixed values of the recoil energy. The main shortcoming of this prediction for $B$ decays is that it only covers recoil energies available in $D$ decays. This is particularly troublesome in the $\pi$ mode, for which most of the rate might be at large recoil energies. It would thus be very useful to have a full calculation of the $B \to \pi\ell\nu$ decay consistent with the constraints from HQS as well as chiral symmetry for heavy hadrons. The information from HQS is contained in the scaling behavior of the form-factors with the heavy masses as well as in the spin symmetry relations for members of the same HQS spin multiplet. In the decays $H \to \pi\ell\nu$, Chiral Perturbation Theory for Heavy Hadrons (CPTHH) [4, 5] promotes nearest singularity (pole) dominance to the leading contribution in the chiral and heavy quark expansions when the pion is soft. The validity of nearest pole dominance in the soft pion limit is not a surprising result given the proximity of the pole to the physical region where the pion recoil is small. However, there is no reason to believe that this is also true at higher recoil momenta. Deviations from the pure pole behavior at pion recoil energies above $\approx$ 1GeV in $B \to \pi\ell\nu$ result in large modifications in the branching ratio. Conversely, the physical region in the case of the $D$ modes is confined to be closer to the pole and therefore one expects the approximation of the form-factors by the single pole to be a rather good one over a large fraction of phase space. In this paper, we construct a model which reflects pole dominance at low pion energies but at the same time includes other

effects that are potentially important, mostly in $B$ decays. These will include the effect of resonances other than the $B^*$-pole as well as the continuum. A natural model emerges from the dispersion relations for the form-factors [6]. Their properties in the physical region are determined not only by the isolated poles but also by the singularities above the $(m_H + m_\pi)^2$ threshold. The contributions from resonances above threshold can be parametrized in a way compatible with HQS. This allows us to fix the parameters of the model in $D$ decays and have a prediction for *all the available phase space* in $B \to \pi\ell\nu$.

Recently CLEO has observed this decay for the first time and measured its branching ratio [7]. It is therefore imperative to realistically assess the theoretical uncertainties associated with this mode and their impact on the extraction of $|V_{ub}|$. The model we present here is an attempt to address this issue. We expect the contributions to the dispersion relations governing these transitions to be highly constrained by chiral symmetry, HQS and perturbative QCD, to the point of having a complete picture of the physics involved and very little freedom. In the next section we discuss the various contributions to the form-factors in $H \to \pi\ell\nu$, with $H = (D, B)$, in the language of dispersion relations. In Section 3 we derive constraints from chiral symmetry, HQS and perturbative QCD which will highly determine those contributions. In Section 4 we present a model that naturally emerges from all the theoretical constraints, discuss its predictions and compare them with other calculations. We summarize our results and conclude in Section 5.

# 2 Dispersion Relations

The hadronic matrix element for the $B^0 \to \pi^-\ell^+\nu$ transition can be written as

$$\langle \pi(\mathbf{p}_\pi)|\bar{u}\gamma_\mu b|H(\mathbf{P})\rangle = f_+(q^2)(P + p_\pi)_\mu + f_-(q^2)(P - p_\pi)_\mu \tag{1}$$

where $q^2 = (P - p_\pi)^2$ is the momentum transferred to the leptons. In the approximation where the leptons are massless, only the form-factor $f_+(q^2)$ enters the partial rate. This form-factor obeys a dispersion relation of the form

$$f_+(t) = \frac{-\gamma}{(m_{H^*}^2 - t)} + \frac{1}{\pi}\int_{s_0}^{\infty} \frac{Im\,[f_+(s)]\,ds}{(s - t - i\epsilon)} \tag{2}$$

where $s_0 = (m_H + m_\pi)^2$. The isolated pole at $m_{H^*} < s_0$ is actually present in the $B$ meson case, whereas for the $D \to \pi$ transition the $D^*$ pole is located almost exactly at threshold. There are no anomalous thresholds in the $H \to \pi\ell\nu$ transitions, although there might be in $H \to \rho\ell\nu$. Contributing to the imaginary part in (2) are all possible intermediate states that couple to $H\pi$ and are annihilated by the weak vertex, as shown schematically in Fig. 1. These include the multiparticle continuum as well as resonances. The latter must be *radially* excited $J^P = 1^-$ states in order to contribute to $f_+(t)$, and are expected to be located at about $\approx 1$ GeV above the ground state [8]. The first contribution appearing above $s_0$ corresponds to the $H^{(*)}\pi$ continuum. Other contributions to the continuum include states with $H^{(*)}$ mesons and various light mesons (e.g. multipion states). We will neglect them at these values of $s$ because they involve higher order terms in the chiral expansion. Finally, we consider the contributions of orbitally excited $H$ mesons with one pion. In principle these could be important given that the $L = 1$, P-wave states are only about $\approx 500$ MeV above the ground state [9]. The lightest $L = 1$ states correspond to $(0^+, 1^+)$ and $(1^+, 2^+)$ doublets. The second doublet, however, does not couple to the ground state to leading order in CPTHH [10]. The doublet $(0^+, 1^+)$ does couple to the ground state doublet, but the vertex $H\pi \to (0^+, 1^+)\pi$ vanishes to leading order. Therefore, not far from threshold, the continuum contribution to the dispersive integral (2) can be approximated by the $H^{(*)}\pi$ intermediate states. We will estimate this contribution in CPTHH in Section 3.1.

The contributions from the radial excitations of the $H^*$ dominate the imaginary part at intermediate values of $s$. Separating them from the continuum one can express (2) as

$$f_+(t) = \frac{-\gamma}{(m_{H^*}^2 - t)} + \frac{1}{\pi}\int_{s_0}^{\Lambda^2} \frac{Im\left[f_+^{\text{cont.}}(s)\right] ds}{(s - t - i\epsilon)} + \sum_i a_i \mathcal{R}_i(t). \tag{3}$$

where the cutoff in the continuum integral defines the maximum center of mass energy in $H\pi$ scattering for which the main contribution comes from the continuum. This also corresponds to the beginning of the resonance-dominated region. Typically, $\Lambda$ defines an energy about 0.7 to 1 GeV above threshold. Therefore, the use of CPTHH to compute the continuum contribution to the dispersive integral is justified.

In the narrow width approximation

$$\mathcal{R}_i(t) \equiv \frac{1}{M_i^2 - t} \tag{4}$$

whereas if finite width effects are taken into account these functions take the form

$$\mathcal{R}_i(t) \equiv \frac{1}{\pi}\left(\frac{\pi}{2} - \arctan\frac{s_0 - M_i^2}{M_i\Gamma_i}\right)\frac{(M_i^2 - t)}{(M_i^2 - t)^2 + M_i^2\Gamma_i^2} \tag{5}$$

with $M_i$ the mass of the $i$-th radial excitation. In deriving (5) the widths $\Gamma_i$ were assumed to be constant. The $a_i$'s are the couplings analogous to $\gamma$ of the nearest resonance $H^*$, the residues at the poles. They involve the strong coupling between the $i$-th resonance and $H\pi$, as well as the decay constant of the resonance.

The physical region for the decay $H \to \pi\ell\nu$ is given by the interval $t = (0, t_{\rm max})$, with $t_{\rm max} = (m_H - m_\pi)^2$. Thus the $H^*$-pole, the first term in (3), corresponds to the singularity closest to this region and will be the dominant contribution for values of $t$ close to $t_{\rm max}$. However, the question of how good this approximation is in each case is not a simple one. For instance, neglecting the continuum contribution, it is likely that the $H^*$-pole approximation will be a good one as long as the three-momentum of the recoiling pion, $p_\pi$, is not larger than $\Delta_1 \equiv M_1 - m_{H^{(*)}}$, the gap between the ground state and the first radially excited state. This intuitive picture suggests that the $H^*$-pole term in (3) should be a reasonable approximation to $f_+(t)$ for $D$ semileptonic decays, given that almost all its phase-space falls in this region. However, this is certainly not the case for $B \to \pi\ell\nu$. Although the spacings between resonances and the ground state are independent of the heavy quark mass to a very good approximation, now the recoil momentum of the pion can be as large as $p_\pi^{\rm max} \approx m_B/2$. As $p_\pi$ increases and we move away from the $H^*$-pole, the relative influence of the higher resonances grows. These deviations from the pure $H^*$-pole behavior at large values of $p_\pi$ are particularly important given that the pion momentum distribution goes as $p_\pi^3$. As we will see below, large changes in the total rate and the shape of the $t$ distribution occur when the corrections to the $H^*$-pole behavior at large $p_\pi$ are taken into account.

In what follows, we will consider the theoretical constraints that can be imposed on $f_+(t)$.

These constitute the basis for a model calculation of the $B \to \pi$ transition form-factor, which will incorporate all of these constraints.

# 3 Theoretical Constraints

Although the form-factor $f_+(t)$ is not calculable in perturbation theory, it must satisfy several constraints. These result from the application of HQS, chiral symmetry and the asymptotic behavior imposed by perturbative QCD for exclusive processes.

## 3.1 Chiral Symmetry

Chiral Perturbation Theory for Heavy Hadrons (CPTHH) provides a formal framework for the approximation that only keeps the first term in (2) [4, 5]. In the effective theory that couples heavy hadrons to goldstone bosons respecting HQS and chiral symmetry, the heavy meson fields are represented by the $4 \times 4$ matrices

$$\mathcal{H} = \frac{(1+\not{v})}{2} \{\not{H}^* - H\gamma_5\} \tag{6}$$

where $H_\mu$ and $H$ are the $1^-$ and $0^-$ ground state fileds respectively, and $v_\mu$ is the heavy meson four-velocity. The goldstone bosons enter through

$$\xi = \exp\left(i\pi(x)_a T_a / f\right) \tag{7}$$

with $T_a$, $(a = 1, \ldots, N^2 - 1)$ the $SU(N)$ generators and $\pi_a(x)$ the goldstone boson fields. To leading order $f = f_\pi$, the pion decay constant. The leading order Lagrangian, invariant under HQS and chiral symmetry, is given by [4, 5]

$$\mathcal{L}_{\text{eff.}} = iTr\left[\bar{\mathcal{H}} v.D \mathcal{H}\right] + gTr\left[\bar{\mathcal{H}} \not{A} \mathcal{H}\gamma_5\right]. \tag{8}$$

The coupling constant $g$ is independent of the heavy mass and the axial-vector field is defined by

$$A_\mu = \frac{-i}{2}\left(\xi^\dagger \partial_\mu \xi - \xi \partial_\mu \xi^\dagger\right). \tag{9}$$

Requiring that the weak current transforms as a left-handed doublet implies

$$J^{\mu}_{\rm weak} = -i\frac{\sqrt{m_H}f_H}{2}Tr\left[\bar{\mathcal{H}}\xi^{\dagger}\gamma^{\mu}(1-\gamma_5)\right] \tag{10}$$

with $f_H$ the heavy pseudoscalar decay constant. This completes the description to leading order both in $1/m_H$ and $1/\Lambda_\chi$, where $\Lambda_\chi$ is the scale of chiral symmetry breaking. The $H \to \pi\ell\nu$ transition receives a direct contribution from (10), as well as an $H^*$-pole term resulting from the $H^*H\pi$ interaction governed by the coupling $g$ in (8) followed by the $H^*$-vacuum transition governed by (10). The latter dominates the former in the $1/m_H$ expansion. Thus, for soft pion momentum, the transition form-factor can be approximated by

$$f_+(t) \simeq -\frac{g\ \ f_H\ \ m_H^2/f_\pi}{(m_H^2-t)}. \tag{11}$$

Therefore, CPTHH tells us that to leading order the form-factor is approximated by the first term in the dispersion relation (2) with

$$\gamma = \frac{g\, f_H\, m_H^2}{f_\pi}. \tag{12}$$

In this way CPTHH provides an approximate normalization of $f_+(t)$ at low pion recoil momentum, $|\vec{p_\pi}| \lesssim 1$GeV.

On the other hand, CPTHH can be used to compute the continuum contribution in (3) for values of the integrand close to threshold. At this values of $s$ unitarity implies

$$Im[f_+^{\rm cont.}(s)] = \sigma(s)\, T^{\dagger}(s)\, f_+(s) \tag{13}$$

where the threshold factor is

$$\sigma(s) \equiv \left(1-\frac{(m_H^2-m_\pi)^2}{s}\right)^{1/2}\left(1-\frac{(m_H^2+m_\pi)^2}{s}\right)^{1/2} \tag{14}$$

and $T(s)$ is the $H\pi \to H\pi$ scattering amplitude projected onto the $J=1$ partial wave. We neglect the contribution of the $H^*\pi$ intermediate state which is suppressed by a factor of

$p_\pi/m_H$ relative to $H\pi$. Therefore, above $s_0$ but below the resonance region in the cut, the phase of $f_+(s)$ is given by the $H\pi \to H\pi$ scattering phase-shift

$$\sin\delta_+(s) = \sigma(s)\ |T(s)|. \tag{15}$$

The computation from (8) is straightforward. After projecting to the correct partial wave and isospin channels the phase, to leading order, is given by

$$\sin\delta_+(s) \simeq -\frac{1}{24\pi}\left(\frac{g}{f_\pi}\right)^2 p_\pi^3 \left(\frac{3}{v.p_\pi - \Delta} + \frac{1}{v.p_\pi + \Delta}\right) \tag{16}$$

where $\Delta \equiv m_{H^*} - m_H$ is the mass splitting within the ground state and

$$v.p_\pi = \frac{s - m_H^2 - m_\pi^2}{2\ m_H} \tag{17}$$

is the pion energy in the $H$ rest frame. The dominant effect, once again, comes from the $H^*$-pole exchange, both in the $s$ and $t$ channels. These are governed by the same coupling $g$ entering in the $H^*H\pi$ vertex in (8), and therefore do not introduce any new parameter. The phase in (16) together with the leading order expression for $|f_+(s)|$ yields $Im[f_+^{\rm cont.}](s)$, in the threshold region. The corresponding dispersive part provides, in a next-to-leading singularity approximation, the first correction to the $H^*$-pole behavior. However, as we will see below, this is not the most important modification to pole dominance coming from the cut. The presence of radially excited states, coupling to both the ground state and the weak current turns out to be a more significant correction.

## 3.2 Heavy Quark Symmetry

Although HQS is an ingredient of the CPTHH formulation, the applicability of the flavor symmetry is very limited in practice, as it was mentioned above, if the scaling of $f_+(t)$ with $m_H$ is used to relate $D \to \pi\ell\nu$ to $B \to \pi\ell\nu$. However, we will show here that the application of HQS to the dispersion relation of (3) does not suffer from such limitations. The first two terms in (3) already have a defined behavior with $m_H$ built in CPTHH. On the other hand,

the residues $a_i$ governing the resonant contributions scale as $m_H^{3/2}$, the same way $\gamma$ does. This allows us to write

$$\frac{a_i}{\gamma} = \frac{g_i}{g}\, r_i \tag{18}$$

where $g_i$ is a dimensionless constant characterizing the coupling of the radially excited resonance $H_i$ to $H^{(*)}\pi$, and $r_i$ is essentially the ratio of the mass independent decay constant of $H_i$ to that of the ground state, $f_H$. On the other hand, the spacing among resonances and also the gap to the ground state is independent of $m_H$, to leading order in the heavy mass. Therefore, if we knew the $a_i$'s and the masses of the resonances for the charm system, we would know $f_+(t)$ for $B \to \pi\ell\nu$ *in the whole physical region*. This is an important departure from the application of the flavor HQS to semileptonic decays. The HQS is applied to the resonances in the cut, which have excitation energies independent of the heavy mass as long as both the $c$ and the $b$ quark are considered to be sufficiently heavy. Of course, we do not know a priori the values of the $a_i$'s and the spacings among resonances and the ground state. The latter can be calculated in potential models that have been successful in predicting the spectrum of the *orbitally* excited heavy mesons [9] and are expected to yield a good approximation also for the radial excitations. Regarding the couplings $a_i$, if the sum in (3) has a small number of terms, we will show below that the asymptotic behavior of $f_+(t)$ plus the $D$ decay data can be used to fix their values, resulting in a fully predictive model for the $B$ decay. This procedure assumes that the effect of the heaviest resonances can be absorbed in the values of the lighter radial excitations in such a way that the "effective" couplings still obey the heavy mass scaling given above. For instance, truncating the sum over resonances at $i = 2$, the effect of the heavier resonances can be absorbed, for instance, by $a_2$, defining

$$a_2^{\text{eff.}} \equiv a_2 + \sum_{i=3} a_i \left(1 - \frac{\delta_i}{v.p_\pi + \Delta_2}\right)\left(1 - \frac{\delta_i}{2m_H}\right) \tag{19}$$

with $\Delta_2 \equiv M_2 - m_H$ and $\delta_i \equiv M_i - M_2$. As long as the spacing between successive resonances becomes smaller, one can neglect $\delta_i/(2m_H)$ corrections. This implies that $a_2^{\text{eff.}}$ has the same $m_H$ dependence as $a_2$ so the $m_H$ scaling is still valid for the truncated case. The interpretation of $a_2^{\text{eff.}}$ is not straightforward. In particular, there is no clear correspondence of this quantity

with the product of the coupling $g_2$ times the decay constant of the resonance $H_2$. This, however, is not a problem as we will fit the effective parameters to data. Before doing so, there is a last theoretical constraint we can impose on $f_+(t)$, regarding its behavior at large values of $|t|$.

### 3.3 Asymptotic Behavior

The behavior of the form-factor $f_+(t)$ for very large values of $|t|$ can be estimated reliably in perturbative QCD for exclusive processes (pQCD) [11]. In this approach the hadronic matrix element is described by the hard scattering transition amplitude folded into an overlap integral between the two hadron state wave-functions. To leading order, the hard scattering amplitude is approximated by the one-gluon exchange diagrams. The gluon momentum satisfies

$$Q^2 = (1-x)^2 m_H^2 + (1-y)^2 m_\pi^2 \pm 2(1-x)(1-y) P \cdot p_\pi \tag{20}$$

where $x$ and $y$ are the momentum fractions of the non-spectator quarks in the initial and final hadron, respectively. The positive sign in the last term in (20) corresponds to the s-channel process $\ell\nu \to H\pi$, whereas the negative signs corresponds to the t-channel, e.g. $\ell H \to \nu\pi$ as well as to the decay $H \to \pi\ell\nu$. In order for pQCD to be safely applicable we need $Q^2 \gg 1\text{GeV}^2$. However, the wave-function of a meson containing a heavy quark peaks at $x \simeq (1-\epsilon)$, with

$$\epsilon \simeq \mathcal{O}\left(\frac{\Lambda_{\text{QCD}}}{m_Q}\right) \tag{21}$$

This implies that in the physical region for the decay $H \to \pi\ell\nu$ the gluon momentum is $Q^2 \lesssim 1\text{GeV}^2$, with the exception of a negligible large-$Q^2$ tail of the wave-function. This casts a serious shadow over the applicability of the one-gluon exchange approximation in computing $f_+(t)$ in the physical region for the semileptonic decay, signaling possible large corrections. However, outside the physical region and for large enough values of $|t|$, the condition $Q^2 \gg 1\text{GeV}^2$ is satisfied. In these two regions, for $t \ll 0$ and for $t$ much larger than the typical mass of heavy resonances, pQCD should yield a very good approximation to the form-factor. The known asymptotic behavior of $f_+(t)$ constitutes an important constraint

to be satisfied by any calculation. We rewrite the dispersion relation as

$$\begin{aligned} f_+(t) &= -\frac{\gamma}{(m_{H^*}^2 - t)} + \frac{1}{\pi}\int_{s_0}^{\Lambda^2} \frac{Im[f_+^{\rm cont.}(s)]ds}{s-t-i\epsilon} + \frac{1}{\pi}\int_{\Lambda^2}^{\Lambda'^2} \frac{Im[f_+(s)]ds}{s-t-i\epsilon} \\ &+ \frac{1}{\pi}\int_{\Lambda'^2}^{\infty} \frac{Im[f_+(s)]ds}{s-t-i\epsilon} \end{aligned} \tag{22}$$

The second term in (22) contains the continuum contribution, whereas the third one accounts for the region dominated by resonances, for $\Lambda^2 < s < \Lambda'^2$. The last term in (22) can be calculated perturbatively provided $\Lambda'$ is sufficiently large. Its contribution is small for values of $t$ in the physical region. At very large $|t|$, for instance for $t \ll 0$, the form-factor can also be calculated perturbatively. Thus, the asymptotic behavior of (22) gives

$$\begin{aligned} f_+(t) &\longrightarrow \frac{-1}{t}\left\{-\gamma + \frac{1}{\pi}\int_{s_0}^{\Lambda^2} Im[f_+^{\rm cont.}(s)]ds + \frac{1}{\pi}\int_{\Lambda^2}^{\Lambda'^2} Im[f_+(s)]ds + p_1(t,\Lambda')\right\} \\ &\longrightarrow f_+^{\rm pQCD}(t) \end{aligned} \tag{23}$$

where the last term in the brackets in (23) is the leading asymptotic contribution from the last term in (22). The non-perturbative contributions in (23) are, *individually*, much larger than $t \times f_+^{\rm pQCD}(t)$. Therefore, because $f_+^{\rm pQCD}(t)$ is a reliable approximation to the form-factor for $t \to -\infty$, there must be large cancellations among the non-perturbative contributions. This leads to a convergence condition or "sum rule" of the form:

$$\gamma - \frac{1}{\pi}\int_{s_0}^{\Lambda^2} Im[f_+^{\rm cont.}(s)]ds - \frac{1}{\pi}\int_{\Lambda^2}^{\Lambda'^2} Im[f_+(s)]ds \simeq 0 \tag{24}$$

where the equality corresponds to $f_+^{\rm pQCD}(t) = -p_1(t,\Lambda')/t$. This sum rule translates our knowledge of the asymptotic behavior of $f_+(t)$ as a constraint on the non-perturbative contributions, which in turn dominate $f_+(t)$ in the physical region. In order to actually implement this constraint, we can write the integral over the resonant region as a sum over the individual resonances. In the narrow width approximation, we have

$$\frac{1}{\pi}\int_{\Lambda^2}^{\Lambda'^2} \frac{Im[f_+(s)]ds}{s-t-i\epsilon} = \sum_{i=1} \frac{a_i}{M_i^2 - t} \tag{25}$$

where the $a_i$'s are defined in Section 2. In this way the convergence condition now reads

$$\gamma - c - \sum_{i=1} a_i \simeq 0 \tag{26}$$

where we defined

$$c \equiv \frac{1}{\pi} \int_{s_0}^{\Lambda^2} Im[f_+^{\text{cont.}}(s)] ds \tag{27}$$

Finite width effects are taken into account by the replacement $a_i \to a_i I_i$, with the $I_i$'s defined by

$$I_i \equiv \frac{1}{\pi} \left( \frac{\pi}{2} - \arctan \frac{s_0 - M_i^2}{M_i \Gamma_i} \right). \tag{28}$$

The convergence relation of (26) is a very binding constraint for model building. In the next section we will explore a specific model for the resonant contribution in order to understand the effect of (26) on the behavior of $f_+(t)$ in the physical region.

# 4 Constrained Dispersive Model of $f_+(t)$

In order to implement the various theoretical constraints from the previous section into a calculation of $f_+(t)$ we need to specify the resonant contributions. First, we must truncate the sum over resonances in (3). As the radial excitations of the H* become heavier, they are less relevant to $f_+(t)$. On the one hand, heavier resonances contribute with a smaller value of $\mathcal{R}_i$ even in the narrow width approximation. Furthermore, as finite widths are considered, the contributions of heavier and thus broader excitations are additionally suppressed, as can be seen in (5). On the other hand, the couplings of the excitations to the ground state, $g_i$, are constrained to obey an Adler-Weisberger sum rule [12]

$$1 \gtrsim g^2 + g_1^2 + g_2^2 + ... \tag{29}$$

where $g_i$ is the coupling the the $i$-th radial excitation to $H\pi$, and additional terms, e.g. from orbitally excited states, are not shown. This implies that one cannot add a large number of resonances in the cut with large couplings to the ground state. This, together with the mass

and width suppression, shows that the truncation of the sum over resonances is a controlled approximation.

In what follows, we will study a Constrained Dispersive Model (CDM) where only the first two terms in the sum over resonances are kept. This is partly motivated by the fact that only two $1^-$ radially excited states are known in the light-quark sector. On the other hand, the "minimal" choice of keeping only one term will turn out to be incompatible with the data on exclusive charm semileptonic decays and the convergence condition (26), as we will see below.

The other necessary ingredient to specify the model is the knowledge of the spectrum of radial excitations. These resonances ((2S) and (3S) excitations of $D^*$ and $B^*$) have not been observed in the $D$ or $B$ systems. We will then rely on potential model calculations of their masses [8]. These models have been very successful in predicting the masses of orbitally excited states, and therefore we are confident that the position of the radial excitations in the cut does not introduce a sizeable uncertainty. The resulting spectrum explicitly shows that the spacings among the 1S, 2S and 3S states are, to leading order, independent of the heavy quark mass and therefore constitute a property of the light degrees of freedom. We take the spectrum of radial excitations to be [8]

$$\begin{array}{lll} M_1^D = 2.7 \text{ GeV} & ; & M_2^D = 3.3 \text{ GeV} \\ M_1^B = 6.1 \text{ GeV} & ; & M_2^B = 6.6 \text{ GeV} \end{array} \tag{30}$$

where the subindex 1 corresponds to the 2S excitation of the $H^*$, etc. In this model, the convergence condition (26) now reads

$$\gamma - c - a_1 - a_2 \simeq 0 \tag{31}$$

This condition, together with eqn. (12) for $\gamma$ and the CPTHH calculation for the continuum term $c$ defined in (27), leaves only one free parameter in the model. This parameter can be fixed by fitting to the observed $D^0 \to \pi^- e^+ \nu_e$ branching ratio. Given that $a_1/\gamma$ and $a_2/\gamma$ are independent of the heavy quark mass, this procedure results in a prediction for $B^0 \to \pi^- \ell^+ \nu$. The result not only has the correct scaling of $f_+(t)$ with the heavy meson mass but also implements the HQS properties of the resonances in the cut, namely the scaling of the $a_i$'s with $m_H$.

The form-factor emerging in this picture has the form

$$f_+(t) = \frac{-\gamma}{m_{H^*}^2 - t}\left(\frac{M_2^2 - m_{H^*}^2}{M_2^2 - t}\right) + \frac{a_1(M_2^2 - M_1^2)}{(M_1^2 - t)(M_2^2 - t)} + \frac{1}{(M_2^2 - t)}\frac{1}{\pi}\int_{s_0}^{\Lambda^2} \frac{(M_2^2 - s) Im[f_+^{\rm cont.}(s)]}{s - t - i\epsilon} ds \qquad (32)$$

where we made use of the narrow width approximation. The cutoff in the integral in (32) is given by $\Lambda \simeq (m_H + 0.7\text{GeV})$, which corresponds to the maximum center-of-mass energy in $H\pi$ scattering for which CPTHH can be used to compute the phase of $f_+(s)$, and at the same time coincides with the beginning of the resonance dominated region in the cut.

In order to fit (32) to the $D^0 \to \pi^- e^+ \nu_e$ data we need values for $f_D$ and $g$ entering in the expression (12) for $\gamma$. Currently there is only an upper limit on the decay constant from $D \to \mu\nu$ , $f_D < 0.310$ GeV [13]. On the other hand, the CLEO collaboration measurement of $D_s \to \mu\nu$ gives $f_{D_s} = (0.284 \pm 0.030 \pm 0.030 \pm 0.016)$ GeV [14]. We combine this with the predictions from lattice calculations [15] for the ratio of decay constants, to obtain the value $f_D = 0.24$ GeV, to be used in the fit. The $H^*$ $H\pi$ coupling gets an upper bound from the upper limit on the $D^*$ lifetime [16] plus the $D^* \to D\pi$ branching fraction [13]. It is also possible to derive a lower limit on $g$ from $D^* \to D\gamma$ [17]. These two combined give $0.3 < g < 0.7$. We take $g = 0.50$ for some of our numerical estimates. Finally, the prediction for $B^0 \to \pi^- \ell^+ \nu$ will depend on the $B$ meson decay constant $f_B$. Lacking experimental information on this quantity, we make use of the scaling with heavy meson masses and, from the value for $f_D$, we obtain $f_B = 0.15$ GeV. In any event the values of $f_D$, $f_B$ and $g$ are external input parameters and not model parameters. Eventually, they will be experimentally determined.

We are now ready to fit (32) to $D^0 \to \pi^- e^+ \nu_e$ and fix the value of $a_1/\gamma$. A recent CLEO measurement [18], combined with the value in [13] for $D^0 \to K^- e^+ \nu_e$, gives $Br^{\rm CLEO}(D^0 \to \pi^- e^+ \nu_e = (3.90 \pm 1.5) \times 10^{-3}$. We do not make use of the more precisely measured $D^0 \to K^- \ell^+ \nu$ mode due to the presence of potentially large $SU(3)$ breaking effects, which we do not take into consideration. Thus, at this point, the largest uncertainty in the model prediction comes from the experimental uncertainty in the $D^0 \to \pi^- e^+ \nu_e$ branching ratio. It is expected

that this will be known to within 5% in the near future [19].

With this choice of external parameters, the form-factor of (32) is shown in the solid line of Fig. 2 for the $B^0 \to \pi^- \ell^+ \nu$ mode. Also shown for comparison, are the first term in the dispersion relations (2) (dashed-line), corresponding to the $B^*$-pole with $\gamma$ given by (12) (chiral $B^*$-pole), as well as the prediction from the BSW model (dotted line) [20]. The pion momentum distributions for these cases are shown in Fig. 3. As expected, the chiral $B^*$-pole is a good approximation to the full form-factor up to pion momenta of $\mathcal{O}(1)$ GeV. Above this momentum, large deviations from the $B^*$-pole behavior are observed. On the other hand, with the choice of parameters made, the model interpolates between the soft momentum region, predicted by CPTHH, and the BSW calculation of the form-factor at $t = 0$. This type of procedure was first suggested in [21]. After all, the relativistic quark model calculation of $f_+(0)$ in the BSW model constitutes the most reliable prediction of quark models for charmless decays of $B$ mesons. Thus, one alternative within our model to the need of knowing the external parameters, is to normalize the prediction in $B \to \pi \ell \nu$ to agree with the prediction from [20] at $t = 0$. As seen in Fig. 3, choosing the central values of all the external parameters provides us with a good extrapolation. On the other hand, the ISGW2 model [22] is a modification of the non-relativistic quark model of [23] which has a harder pion momentum spectrum than the original calculation in order to give a better fit to the pion electromagnetic form-factor $F_\pi(Q^2)$. Thus the shape of the spectrum in the ISGW2 model is a parametrization of the soft physics governing $F_\pi$. The *shape* of the resulting $f_+(t)$ resembles the one obtained in our calculation and is yet another reason to believe that the convergence relation captures the correct physics at large values of $t$. In the future, the precise measurement of $g$, $f_D$ and $f_B$ will provide an independent prediction whithin our model and will help us understand the relation between this simple dispersive approach and quark models.

We now address the possible sources of corrections to this calculation of the form-factor. The widths of the resonances are expected to be rather large. When finite width effects are taken into account, the form-factor is that given by (3) keeping only the first two terms in

the sum over resonances, with $\mathcal{R}_{1,2}$ given by (5) and the convergence relation

$$\gamma - c - a_1 I_1 - a_2 I_2 \simeq 0, \tag{33}$$

where $I_1$ and $I_2$ are defined by (28). The widths $\Gamma_1$ and $\Gamma_2$ are, in principle, not fixed. However, they can be estimated by calculating the partial widths to the ground state as well as to orbital excitations. To leading order in CPTHH, these interactions are governed by

$$\mathcal{L} = \sum_{i=1}^{2} g_i Tr[\bar{\mathcal{E}}_i \not{A} \mathcal{H} \gamma_5] + \sum_{i=1}^{2} f_i Tr[\bar{\mathcal{E}}_i \not{A} \mathcal{S} \gamma_5] \tag{34}$$

where $\mathcal{H}$ is defined in (6) and represents the ground state doublet, $\mathcal{E}_i$ represent the two radial excitation doublets and have the same form as $\mathcal{H}$, and the $(0^+, 1^+)$ P-wave doublet is given by [10]

$$\mathcal{S} \equiv \frac{(1+\not{v})}{2}[\not{S}\gamma_5 - S_0^*] \tag{35}$$

with $S_0^*$ and $S_\mu$ the $0^+$ and $1^+$ fields respectively. The couplings $g_1$, $g_2$, $f_1$ and $f_2$ are unknown. In order to obtain a conservative estimate of the widths we take the values $g_1 = g_2 = f_1 = f_2 = 0.50$. This choice will probably result in an overestimate of the widths given it does not respect the condition (29). Finally, we account for the the softening of the vertices with momentum by the factor [9]

$$e^{-p_\pi^2/\kappa^2} \frac{1}{(1 + p_\pi^2/m_\rho^2)} \tag{36}$$

where $\kappa$ is a typical hadronic scale $\mathcal{O}(1)$ GeV. This results in

$$\begin{array}{lcl} \Gamma_1^D \simeq (0.25 - 0.35) \text{ GeV} & ; & \Gamma_2^D \simeq (0.40 - 0.50) \text{ GeV} \\ \Gamma_1^B \simeq (0.30 - 0.40) \text{ GeV} & ; & \Gamma_2^B \simeq (0.40 - 0.50) \text{ GeV} \end{array} \tag{37}$$

The resulting prediction for the pion momentum distribution in $B^0 \to \pi^- \ell^+ \nu$ is given by the dashed line in Fig. 4, together with the narrow width approximation result. The reason for the effect being small lies on the fact that, when the widths are incorporated into the fit of the model to the $D^0 \to \pi^- \ell^+ \nu$ branching ratio, the heavy mass independent parameter $a_1/\gamma$

must be slightly modified to upset the width effect. Thus the same type of cancellation takes place in the $B \to \pi\ell\nu$ case. The procedure to obtain a prediction for the $B \to \pi$ transition is built in a way that is nearly independent of the widths. The model dependence on the cutoff $\Lambda$ in the continuum integral is also marginally small. This is partly because of the fitting to the charm meson decay data, but mostly because the continuum plays a small role overall. Finally, we must address violation to the heavy mass independence of the ratios $a_i/\gamma$. The heavy mass dependence in these couplings can be written as

$$\begin{aligned} a_i &\simeq m_H^{3/2}\left(1+\frac{\alpha_i}{m_H}+...\right) \\ \gamma &\simeq m_H^{3/2}\left(1+\frac{\beta}{m_H}+...\right) \end{aligned}$$

Implying

$$\frac{a_i}{\gamma} \simeq N\left(1+\frac{(\alpha_i-\beta)}{m_H}+...\right) \tag{38}$$

with $N$ independent of $m_H$. Therefore potentially large $1/m_H$ corrections partially cancel in $a_i/\gamma$ and the use of the flavor HQS in the branch cut is likely to be a very good approximation.

In Fig. 5 we show the pion momentum distribution for the $D^0 \to \pi^-\ell^+\nu$ decay. The solid line represents the CDM prediction, whereas the dashed line corresponds to the chiral pole term and the dotted line is the BSW model. The CDM prediction agrees well with both, the first term in the dispersion relations and the BSW model. The maximum pion momentum is not large enough to cause a disagreement, which arises at $p_\pi \gtrsim 1$ GeV and to which only the CDM model is sensitive.

As stated above, our results depend on the external parameters $g$, $f_D$, $f_B$ and $Br^{D\to\pi}$, the $D^0 \to \pi\ell^+\nu$ branching ratio. In Table I we present the results for the $B^0 \to \pi^-\ell^+\nu$ branching ratio in units of $|V_{ub}|^2$ for a particular choice of these external parameters and for two sets of masses for the resonances, as well as for the finite width case. The set of radial excitation masses we call Set 1 is the one presented in the text, whereas Set 2 corresponds to a shift of +100 MeV in the masses. As it can be seen, the result is rather stable under these type of modifications. In Table 2 we show results in the narrow width approximation

for $f_D = 0.24$ GeV and for various values of $g$ and $f_B$. As expected, the predicted branching ratio is rather sensitive to the values of these two external parameters, which hopefully will be determined in the near future by experiment and/or lattice calculations.

Although the normalization of the model prediction for $B^0 \to \pi^- \ell^+ \nu$ depends on poorly known or still unmeasured quantities, one characteristic feature of the model that emerges independently of these is the shape of the momentum distribution. As is seen in Figs. 3 and 4, at pion momenta above $\approx 1$ GeV the CDM model predicts that the distribution flattens out, as opposed to the characteristic almost-linear growth of the pure $B^*$-pole behavior. In particular, the CDM prediction for the shape at maximum recoil momentum ($q^2 = 0$) is consistent with the *shape* of the perturbative form-factor in the Brodsky-Lepage formalism. Considering that the CDM shape is a result of imposing the perturbative behavior in the asymptotic region, e.g. for large $-q^2$, this coincidence is interesting and deserves to be studied further. We expect the shape of the pion momentum distribution to be greatly constrained by the future CLEO data [24]. This will allow to discriminate between the CDM approach and the pure $B^*$-pole model. From Table 1 it can be seen that the intrinsic uncertainty of the model is small. This is due to the fact that each change in a model parameter leads to a new value of $a_1/\gamma$ to keep a good fit of $Br^{D\to\pi}$. This procedure, built in the model, makes the predictions for $B^0 \to \pi^- \ell^+ \nu$ very stable. However, an extraction of $|V_{ub}|$ from the CLEO data is not possible at this point given the large uncertainties in external parameters, namely $g$, $f_B$ and $Br^{D\to\pi}$.

# 5 Conclusions

We have presented an approach to semileptonic form-factors that bridges the gap between low and high pion momentum recoil. The dispersion relation described in Section 2 is a suitable framework to identify the various contributions. Furthermore, the imposition of model-independent theoretical constraints leads to either complete calculations or an important reduction in model dependence in calculating the various pieces entering in these transitions.

First, chiral symmetry tells us that , for $p_\pi \lesssim 1$ GeV, the first term in the dispersion

relation (2) is a good approximation to $f_+(t)$, with $\gamma$ given by (12). The singularity closest to this region of the $H \to \pi\ell\nu$ decay is the leading term entering in $f_+(t)$ in CPTHH. The next contribution to (2) comes from the $H^{(*)}\pi$ continuum, which dominates the $Im[f_+(s)]$ from threshold (the branch point) up to a scale where individual resonances start dominating. The phase of $f_+(s)$ in this region is computed in CPTHH, which is a valid tool up to this energy scale. We conclude that the resulting contribution is not the chief modification of the $H^*$-pole behavior.

On the other hand, the radial excitations dominate the $Im[f_+(s)]$ above the scale $\Lambda$, and result in large deviations from the $H^*$-pole behavior at values of $p_\pi$ larger than $\simeq 1$ GeV. Their contributions to the branch cut obey a definite HQS scaling with $m_H$. This imposes a constraint that allows us to relate the $B \to \pi\ell\nu$ form-factor to that entering in the $D \to \pi\ell\nu$ mode for *all values of the pion momentum*. This represents a considerable improvement over the simple $m_H$ scaling of the form-factors, which only allows a prediction of the $B$ mode up to pion momenta smaller than 1 GeV.

Finally, requiring that the form-factor has the correct asymptotic behavior as dictated by perturbative QCD, we derive the convergence relation or sum rule of (24). This translates into an additional constraint to be obeyed by the couplings of the radial excitations, as seen in (26).

The model presented in Section 4 has two active resonances in the branch cut, leaving only one free parameter, which is fixed by fitting to the observed $Br^{D\to\pi}$. The resulting form-factor, as seen for instance in (32) in the narrow width approximation, presents several interesting features. Firstly, it respects the constraints from chiral symmetry, HQS and perturbative QCD. Secondly, it is a realization of the intuitive idea that the $H^*$-pole behavior must be softened by an effective suppression of the coupling $\gamma$. In our model this suppression is provided by the radial excitations in (32). This can be readily seen if we write the first term in (32) as

$$\frac{\gamma}{m_{H^*}^2 - t}\left(\frac{M_i^2 - m_{H^*}^2}{M_i^2 - t}\right) \simeq \frac{\gamma}{m_{H^*}^2 - t}\left(\frac{1}{1 + v.p_\pi/\Delta_i}\right) \tag{39}$$

where $\Delta_i \equiv M_i - m_H$ is the gap between the ground state and the $i$-th excitation, and

provides the scale of suppression which in this case is of about $(0.8-1)$ GeV. Therefore the resonances in the cut give the scale for the effective suppression of the $H^*$-pole behavior at large pion recoil. The model presents a natural explanation for the softening of $\gamma$ [21, 25]. It also provides us with a simple rule for the validity of pole dominance in semileptonic transitions in general: nearest pole dominance is a good approximation for values of the hadronic recoil energy small compared to the gap between the first excitations of the pole and the ground state. This is the reason why pole dominance is a good approximation in $D$ semileptonic decays as well as in $B \to D^{(*)}\ell\nu$ decays, but not in $B \to \pi\ell\nu$, where large portions of the rate come from $v.p_\pi > \Delta_i$.

As discussed in Section 4, the intrinsic uncertainty of the model is small. This implies that a determination of $|V_{ub}|$ from the measurement of the $B \to \pi\ell\nu$ branching ratio will only be limited by the experimental precision with which $Br(D \to \pi\ell\nu)$, $g$, $f_D$ and $f_B$ are determined.

The shape of the pion momentum distribution is a very distinctive feature of the model, as can be appreciated in Figs. 3 and 4. The comparison with the $B^*$-pole as normalized in CPTHH confirms that pole dominance is a good approximation for $p_\pi \lesssim 1$ GeV. However, at larger values of $p_\pi$ the model deviates largely from the characteristic $B^*$-pole distribution. For the same normalization at low $p_\pi$, the branching ratio is about a factor of two smaller than if the pure $B^*$-pole is assumed. The flat distribution at large pion momentum is a consequence of the cancellations that result when imposing perturbative QCD as the asymptotic behavior. Interestingly, this shape resembles the one that is obtained by computing the form-factor directly in perturbative QCD for exclusive processes, characteristic of a dipole fall-off with $t$ [26], rather than a monopole. Although, as we argued in Section 3.3, the pQCD formalism is not expected to give the right answer, this coincidence in shape is an important point to bear in mind in an attempt to fully match the non-perturbative and perturbative regimes. Present and future CLEO measurements of the pion momentum distribution will test this aspect of the model, independently of the values of external parameters.

Another important test of this approach and the natural next step, is the prediction of $B \to \rho\ell\nu$. In this case the constraints from chiral symmetry are not so clear. However,

the HQS and perturbative QCD are still present and largely define the behavior of the form-factors, as in the $B \to \pi\ell\nu$ case. Understanding the $B \to \rho\ell\nu$ to $B \to \pi\ell\nu$ ratio of branching ratios, as well as the polarization in the vector mode will turn into a definite test of this approach and a major step towards the extraction of $|V_{ub}|$ from exclusive decays in the coming $B$ factory era.

# Acknowledgments

The authors thank W. A. Bardeen, J. F. Donoghue, E. Eichten, L. Gibbons, C. Quigg, J. Simone and S. Willenbrock for useful discussions and suggestions. G.B. acknowledges the support of the U.S. Department of Energy. J.K. acknowledges support from the University of Massachusetts, Amherst.

# References

[1] N. Isgur and M. B. Wise, Phys. Lett. **B232**, 113 (1989); *ibid* **B237**, 527 (1990). For a review see M. Neubert, Phys. Rep. **245**, 259 (1994).

[2] M. Luke, Phys. Lett. **B252**, 447 (1990); M. Neubert, Phys. Lett. **B341**, 367 (1995).

[3] I. I. Bigi, M. Shifman, N. G. Uraltsev and A. Vainshtein, Phys. Rev. Lett. **71**, 496 (1993); A. Manohar and M. B. Wise, Phys. Rev. **D49**, 1310 (1994); M. Luke and M. Savage, Phys. lett. **B321**, 88 (1994).

[4] M.B. Wise, Phys. Rev. **D45**, 2188 (1992).

[5] G. Burdman and J.F. Donoghue, Phys. Lett. **B280**, 287 (1992).

[6] Our approach is entirely different from that of C. Boyd, B. Grinstein and R. Lebed, Phys. Rev. Lett. **74**, 4603 (1995). In this reference, bounds on the form-factors are derived by computing a two-point function in pQCD at $q^2 = 16$ GeV$^2$. However, at these values of $q^2$, large corrections are likely to exist that would affect the bounds. On the other hand, computing at large *space-like* values of $q^2$, where pQCD should be

trusted the most in the computation of the vacuum polarization involved, considerably loosens the bounds.

[7] R. Ammar *et al.*, the CLEO collaboration, CLEO CONF 95 09, EPS0165.

[8] E. Eichten, C. T. Hill and C. Quigg, FERMILAB-CONF-94/117-T, published in the Proceeding of the CHARM2000 Workshop, Fermilab, June 1994.

[9] E. Eichten, C. T. Hill and C. Quigg, Phys. Rev. Lett. **71**, 4116 (1993); and FERMILAB-CONF-94/118-T, published in the Proceeding of the CHARM2000 Workshop, Fermilab, June 1994.

[10] A. Falk and M. Luke, Phys. Lett. **B292**, 119 (1992).

[11] G. P. Lepage and S. J. Brodsky, Phys. Lett. **B87**, 959 (1979) and Phys. Rev. **D22**, 2157 (1980). The first application to $B$ decays is found in A. Szczepaniak, E. M. Henley and S. J. Brodsky, Phys. Lett. **B243**, 287 (1990).

[12] C. A. Dominguez and N. Paver, Z. Phys. **C41**, 217 (1988); N. Paver and Riazuddin, Phys. Lett. **B320**, 364 (1994) and C. Chow and D. Pirjol, CLNS 95/1377.

[13] Particle Data Group, Phys. Rev. **D50**, 1173 (1994).

[14] D. Gibaut *et al.*, the CLEO collaboration, CLEO CONF 95-22, EPS0184.

[15] R. M. Baxter *et al.*, the UKQCD collaboration, Phys. Rev. **D49**, 1594 (1994); C. W. Bernard, J. N. Labrenz and A. Soni, Phys. Rev. **D49**, 2536 (1994). For an update see C. Allton, Rome-95/1114, to be published in the proceedings of *Lattice '95*, Melbourne, Australia, July 1995.

[16] S. Barlag *et al.*, the ACCMOR collaboration, Phys. Lett. **B278**, 480 (1992).

[17] J. F. Amundson *et al.*, Phys. Lett. **B296**, 415 (1992).

[18] F. Butler *et al.*, the CLEO collaboration, CLNS 95/1324, CLEO 95-3.

[19] W. E. Johns, private communication.

[20] M. Wirbel, B. Stech and M. Bauer, Z. Phys. **C29**, 637 (1985).

[21] G. Burdman and J.F. Donoghue, Phys. Rev. Lett. **68**, 2887 (1992).

[22] N. Isgur and D. Scora, Phys. Rev. **D52**, 2783 (1995).

[23] N. Isgur, D. Scora, B. Grinstein and M. B. Wise, Phys. Rev. **D39**, 799 (1989).

[24] L. Gibbons, private communication.

[25] N. Isgur and M. B. Wise, Phys. Rev. **D41**, 151 (1990).

[26] G. Burdman and J. F. Donoghue, Phys. Lett. **B270**, 55 (1991). For a more detailed discussion see G. Burdman, UMI-94-08259-mc, 1993, Ph.D. Thesis.

## Tables

| | $Br(B^0 \to \pi^- \ell^+ \nu)/\|V_{ub}\|^2$ |
|---|---|
| NWA (Set 1) | 14.00 |
| NWA (Set 2) | 14.40 |
| FW (Set 1) | 13.40 |

Table 1: CDM prediction of the $Br(B^0 \to \pi^- \ell^+ \nu)$ for $g = 0.50$, $f_D = 0.24$ GeV and $f_B = 0.15$ GeV. Set 1 corresponds to the spectrum of radial excitations of (30) , whereas Set 2 is obtained by a common shift of +100 MeV. The two first results are in the narrow width approximation. The third one includes the effects of the widths as discussed in Section 4, with widths given by (37).

| | $Br(B^0 \to \pi^- \ell^+ \nu)/\|V_{ub}\|^2$ | |
|---|---|---|
| $g$ | $f_B = 0.15$ GeV | $f_B = 0.20$ GeV |
| 0.30 | 19.50 | 35.00 |
| 0.50 | 14.00 | 25.00 |
| 0.70 | 7.30 | 14.00 |

Table 2: CDM prediction of the $Br(B^0 \to \pi^- \ell^+ \nu)$ in the narrow width approximation, for $f_D = 0.24$ GeV and with the Set 1 of radial excitation masses. The values chosen for $g$ cover the allowed region. The results are shown for two typical values of $f_B$.

# Figure Captions

Figure 1: Contributions to the imaginary part of the $H \to \pi\ell\nu$ form-factor $f_+(t)$. The squares represent the action of the weak current and the circles imply strong interactions. The dashed lines are pions and the solid lines are pseudoscalar heavy mesons $H$ unless indicated otherwise.

Figure 2: The form-factor $f_+(t)$ as a function of the momentum transfer $t$. The solid line is the CDM prediction for $g = 0.5$, $f_D = 0.24$ GeV, $f_B = 0.15$ GeV and $Br^{D\to\pi} = 3.9 \times 10^{-3}$. The dashed line is the $B^*$-pole prediction as normalized by CPTHH in (12) (chiral pole) and corresponds to the first term in the dispersion relation (2). The dotted line is the BSW model prediction of Ref. [20].

Figure 3: The pion momentum distribution in units of $|V_{ub}|^2$ as a function of the pion momentum. The caption is the same as in Fig. 2.

Figure 4: The pion momentum distribution in units of $|V_{ub}|^2$ as a function of the pion momentum. The solid line is the CDM prediction in the narrow width approximation. The dashed line is the result taking into account finite widths, as given by (37).

Figure 5: The pion momentum distribution in $D^0 \to \pi^-\ell^+\nu$ as a function of the pion momentum. The solid line is the CDM fit to $Br^{D\to\pi} = 3.9 \times 10^{-3}$ for $g = 0.5$ and $f_D = 0.24$ GeV. Also shown are the chiral pole (dashed line) and the BSW prediction (dotted line).

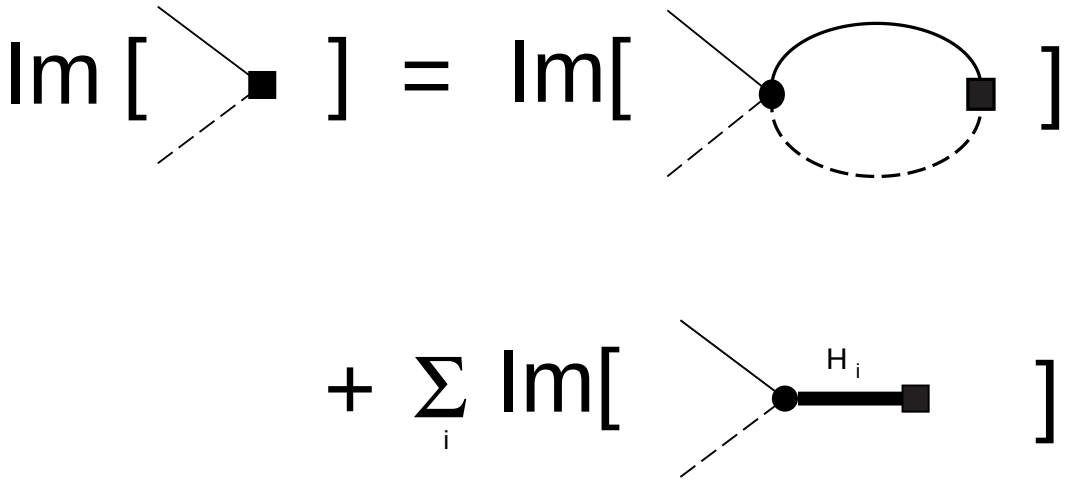


**Figure 1**

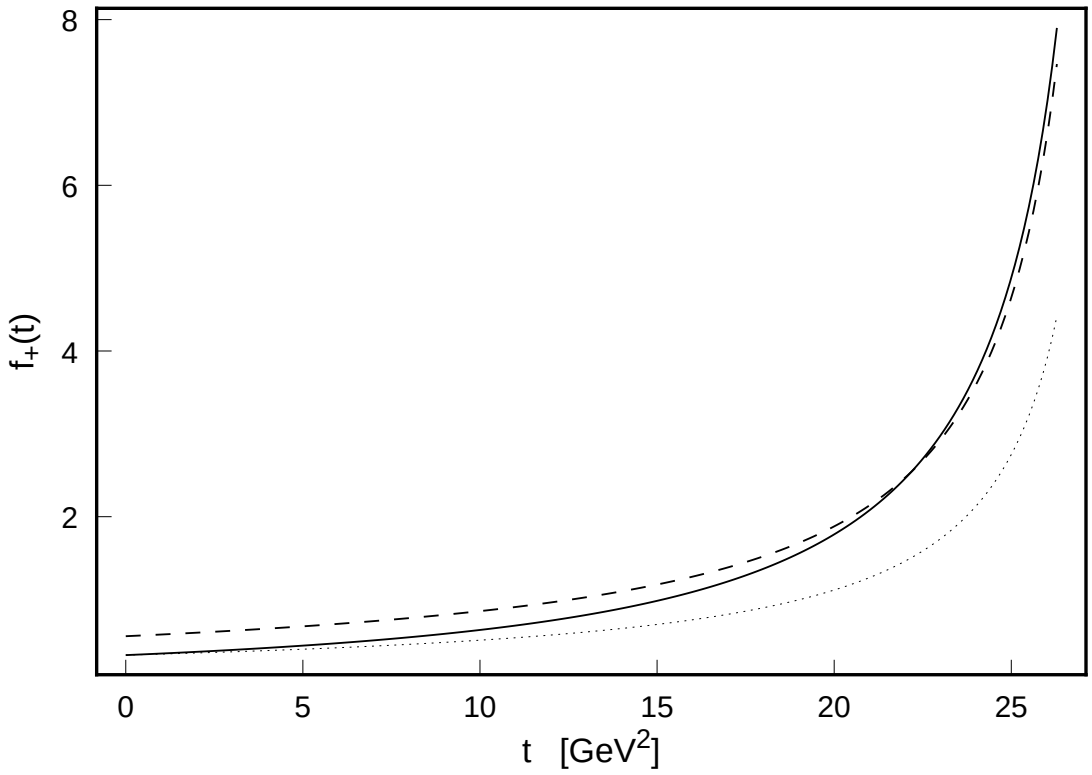


**Figure 2**

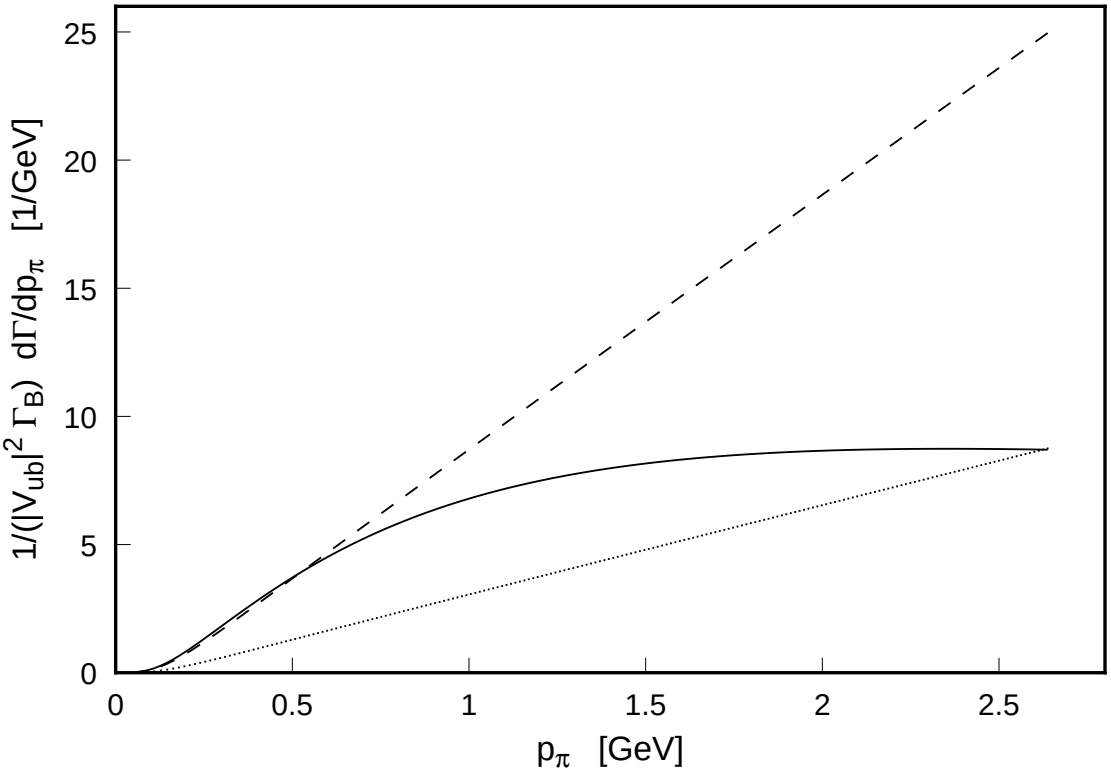
25
20
15
10
5
0
0
0.5
1
1.5
2
2.5
$1/(|V_{ub}|^2\,\Gamma_B)\;\; d\Gamma/dp_\pi$ [1/GeV]
$p_\pi$ [GeV]

**Figure 3**

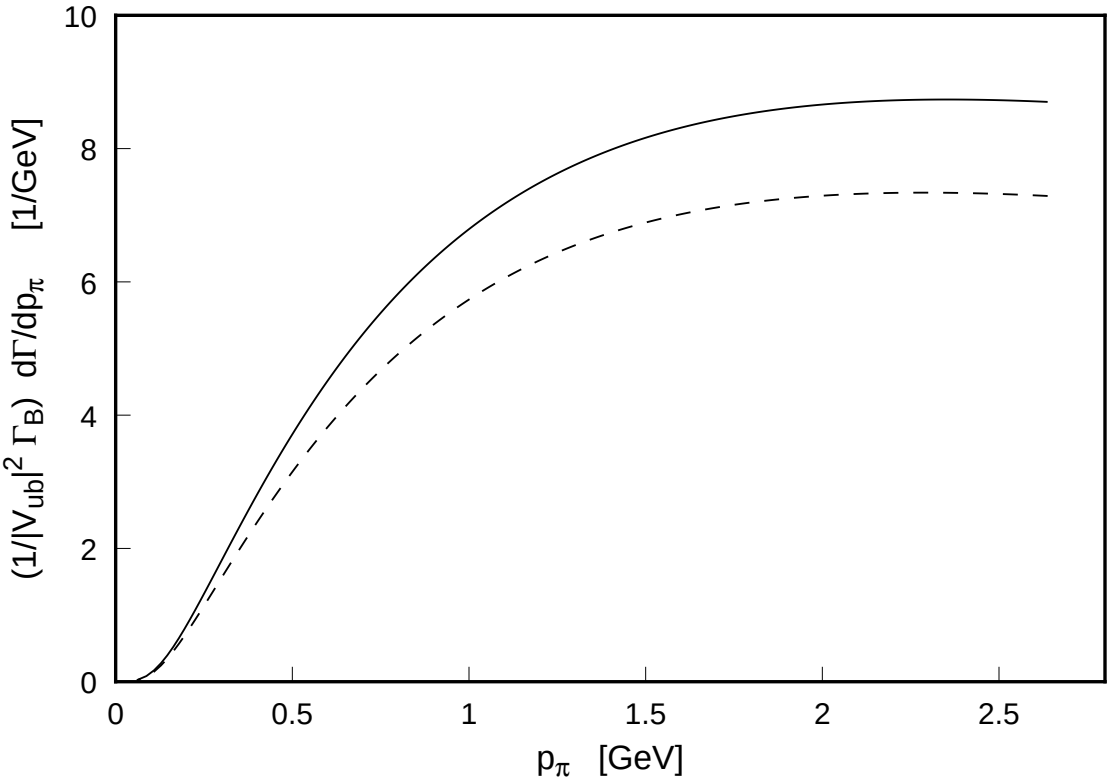


**Figure 4**

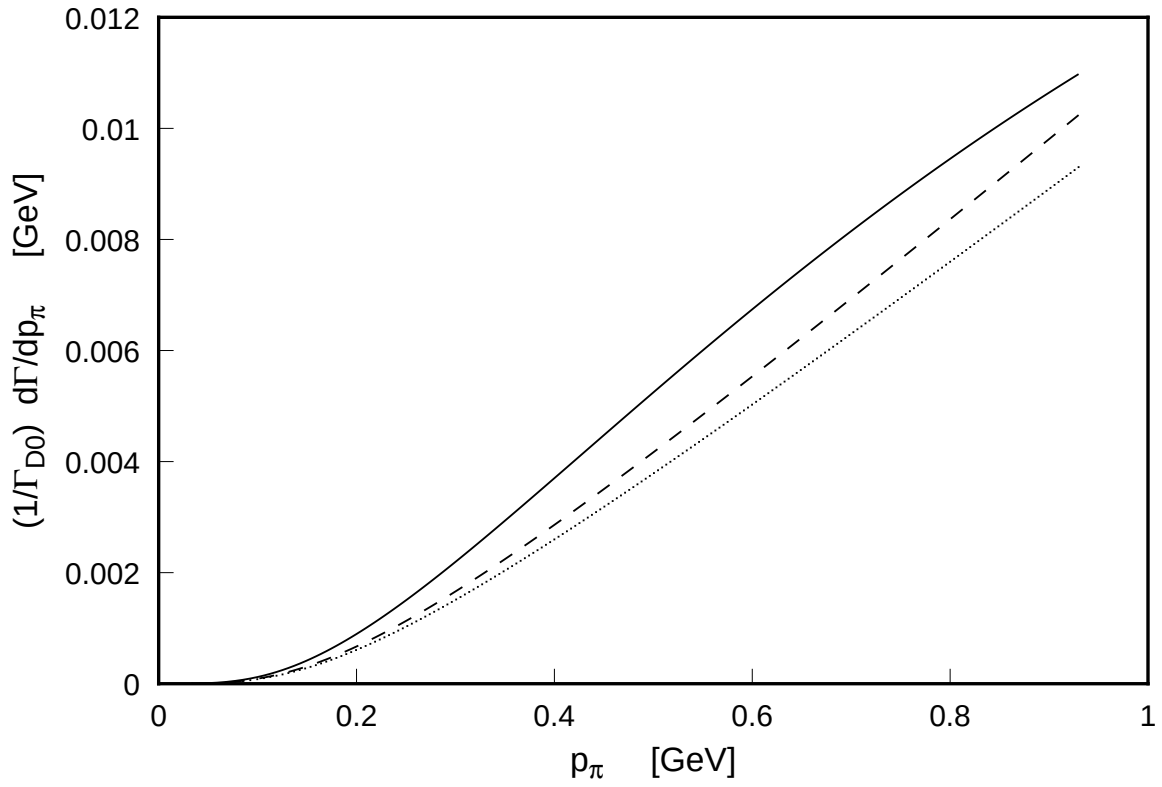
0.012
0.01
0.008
0.006
0.004
0.002
0
0
0.2
0.4
0.6
0.8
1
(1/Γ_D0) dΓ/dp_π [GeV]
p_π [GeV]

**Figure 5**